Integrated analysis of the transcriptome-wide m6A methylome in preeclampsia and healthy control placentas

Jin Wang [1], **Fengchun Gao** [2], **Xiaohan Zhao** [1], **Yan Cai** [1], **Hua Jin** [Corresp. 1]

[1] Prenatal Diagnosis Center, Jinan Maternal and Child Health Care Hospital, Jinan, China

[2] Obstetrical Department, Jinan Maternal and Child Health Care Hospital, Jinan, China

Corresponding Author: Hua Jin
Email address: wangjinshiyi@126.com

N6-methyladenosine (m6A) is the most prevalent modification in eukaryotic mRNA and potential regulatory functions of m6A have been shown by mapping the RNA m6A modification landscape. M6A modification in active gene regulation manifests itself as altered methylation profiles. The number of reports regarding to the profiling of m6A modification and its potential role in the placenta of preeclampsia (PE) is a little. In this work, placental samples were collected from PE and control patients. Expression of m6A-related genes was investigated using quantitative real-time PCR. MeRIP-seq and RNA-seq were performed to detect m6A methylation and mRNA expression profiles. Gene ontology (GO) functional and Kyoto encyclopedia of genes and genomes (KEGG) pathway analyses were also conducted to explore the modified genes and their clinical significance. Our findings show that METTL3 and METTL14 were up-regulated in PE. In total, 685 m6A peaks were differentially expressed as determined by MeRIP-seq. Altered peaks of m6A-modified transcripts were primarily associated with nitrogen compound metabolic process, positive regulation of vascular-associated smooth muscle cell migration, and endoplasmic reticulum organisation. The m6A hyper-methylated genes of Wnt/β-catenin signalling pathway, mTOR signalling pathway, and several cancer-related pathways may contribute to PE. We also verified that the significant increase of *HSPA1A* mRNA and protein expression was regulated by m6A modification, suggesting m6A plays a key role in the regulation of gene expression. Our data provide novel information regarding m6A modification alterations in PE and help our understanding of the pathogenesis of PE.

1 **Integrated analysis of the transcriptome-wide m6A**

2 **methylome in preeclampsia and healthy control**

3 **placentas**

4

5 **Jin Wang[1], Fengchun Gao[2], Xiaohan Zhao[1], Yan Cai[1], Hua Jin[*,1]**

6

7 [1]Prenatal Diagnosis Center, Jinan Maternal and Child Health Care Hospital, Jinan,

8 Shandong Province, PR China

9 [2]Obstetrical Department, Jinan Maternal and Child Health Care Hospital, Jinan,

10 Shandong Province, PR China

11

12 * Corresponding Author:

13 Hua Jin

14 No.2, Jianguo xiaojing roud, Jinan 250002, Shandong Province, PR China

15 Email address: wangjinshiyi@126.com

Abstract

16 **Abstract**

17 N6-methyladenosine (m6A) is the most prevalent modification in eukaryotic mRNA and

18 potential regulatory functions of m6A have been shown by mapping the RNA m6A

19 modification landscape. M6A modification in active gene regulation manifests itself as

20 altered methylation profiles. The number of reports regarding to the profiling of m6A

21 modification and its potential role in the placenta of preeclampsia (PE) is a little. In this

22 work, placental samples were collected from PE and control patients. Expression of

23 m6A-related genes was investigated using quantitative real-time PCR. MeRIP-seq and

24 RNA-seq were performed to detect m6A methylation and mRNA expression profiles.

25 Gene ontology (GO) functional and Kyoto encyclopedia of genes and genomes (KEGG)

26 pathway analyses were also conducted to explore the modified genes and their clinical

27 significance. Our findings show that METTL3 and METTL14 were up-regulated in PE. In

28 total, 685 m6A peaks were differentially expressed as determined by MeRIP-seq. Altered

29 peaks of m6A-modified transcripts were primarily associated with nitrogen compound

30 metabolic process, positive regulation of vascular-associated smooth muscle cell

31 migration, and endoplasmic reticulum organisation. The m6A hyper-methylated genes of

32 Wnt/β-catenin signalling pathway, mTOR signalling pathway, and several cancer-related

33 pathways may contribute to PE. We also verified that the significant increase of *HSPA1A*

34 mRNA and protein expression was regulated by m6A modification, suggesting m6A

35 plays a key role in the regulation of gene expression. Our data provide novel information

36 regarding m6A modification alterations in PE and help our understanding of the

37   pathogenesis of PE.

38   **Introduction**

39   Preeclampsia (PE) is a multi-system disorder that is primarily characterised by new-

40   onset hypertension accompanied by proteinuria during gestation. This disease affects 3–

41   5% of all pregnancies and is one of the leading causes of maternal and perinatal

42   morbidity and mortality (Mol et al. 2016). The exact pathophysiology that causes PE

43   remains unclear; however, genetic, immunological, endocrine, and environmental factors

44   have been implicated in its pathogenesis (Burton et al. 2019). The placenta plays an

45   essential role in the development of PE. The underlying pathogenic mechanisms include

46   defective deep placentation, oxidative and endoplasmic reticulum stress, intravascular

47   inflammation, and imbalance of angiogenesis, among others (Burton et al. 2019;

48   Chaiworapongsa et al. 2014). No specific treatment is currently available, and delivery of

49   the placenta is the only effective treatment (Burton et al. 2019; Chaiworapongsa et al.

50   2014; Wang et al. 2019).

51   Numerous studies have reported that PE significantly alters the expression of

52   coding and noncoding RNAs (ncRNAs), including mRNA, miRNA, long noncoding RNA

53   (lncRNA), and circular RNA (circRNA) (Bai et al. 2018; Liu et al. 2017b; Muller-Deile et al.

54   2018; Nikuei et al. 2017). However, while these studies explored RNA expression, the

55   modification profiles of these RNAs in the context of PE remain to be characterised. N6-

56   methyladenosine (m6A) modification in mRNA is prevalent, and functionally modulates

57   in eukaryotes that is mediated by the m6A methyltransferase complex,

58 methyltransferase-like (METTL)3, METTL14, and Wilms' tumour 1-associated protein

59 (WTAP) and eliminated by fat-mass and obesity-associated protein (FTO) or alkylation

60 repair homolog protein 5 (ALKBH5) (Boccaletto et al. 2018; Fu et al. 2014; Meyer &

61 Jaffrey 2014). These modifications are believed to moderate RNA structure, function,

62 and stability (Edupuganti et al. 2017; Liu et al. 2017a; Piao et al. 2017; Wang et al. 2014).

63 Recently, the effects of m6A modification on many fundamental biological processes

64 have been characterised; these processes include metabolism (Yang et al. 2018),

65 immunomodulation (Zheng et al. 2017), carcinogenesis(Ma et al. 2017; Zhang et al.

66 2017a), and spermatogenesis (Chen et al. 2017), among others. Abnormal m6A

67 methylation is associated with a variety of human diseases, such as obesity, neuronal

68 disorders, cancer, and infertility (Chen et al. 2017; Ma et al. 2017; Yang et al. 2018;

69 Zhang et al. 2017a; Zheng et al. 2017).

70   Given the indispensable function of RNA m6A modification in various bioprocesses,

71 it is reasonable to speculate that deregulation of m6A modification may also be

72 associated with PE. A recent study indicate that m6A at 5'-UTR and nearby stop codon

73 in placental mRNA may play important roles in fetal growth and PE through conducted

74 MeRIP-Seq on human placentas obtained from mothers of infants of various birth

75 weights (Taniguchi et al. 2020). Here, we aimed to compare the m6A-tagged transcript

76 profiles of placentas from PE-affected pregnancies with those of placentas from healthy

77 pregnancies to identify gene-specific changes in RNA methylation that may regulate

78 placental gene expression and contribute to the development of PE. Additionally,

79 potential roles for the m6A-modified transcripts in the physiological and pathological

80 mechanisms underlying PE were revealed; these can provide a theoretical basis for the

81 prevention and pre-emptive treatment of PE.

Materials & Methods

Sample collection

84   All placental samples used in this study were collected from the Department of

85 Obstetrics, Jinan Maternal and Child Health Care Hospital. The characteristics of

86 puerperants and newborns were collected from hospital medical records. PE cases (n =4)

87 were   collected in light of the guideline designed by the American College of Obstetrics

88 and Gynecology (ACOG) (2019; Magee et al. 2014). These cases included women who

89 exhibited a blood pressure of ≥140/90 mmHg on two occasions that occurred at least 4 h

90 apart, accompanied by proteinuria (2+ on dipstick or 300 mg/24 h) at ≥20 weeks and <34

91 weeks of gestation. Normal controls (n =4) were defined as pregnancies without PE. All

92 participants were of Han Chinese descent and those with complications such as

93 gestational hypertension, gestational diabetes mellitus, foetal growth restriction, or

94 preterm birth (<37 weeks) were excluded (Table 1). The study protocols were approved

95 by the Ethics Review Committee of Ji'nan Maternal and Child Health Care Hospital and

96 conducted in accordance with the Declaration of Helsinki (No. JNFY-2019003).

97   Placental samples were collected at three sites from the foetal side of the placenta

98 immediately after caesarean section (<30 min). Fragments of approximately 1 cm^3 were

99 dissected from the placenta after removing maternal blood by vigorous washing in ice-

100 cold saline; these fragments were snap-frozen in liquid nitrogen and stored at -80°C until

101 use. All participants provided written informed consent prior to participation.

102 **RNA isolation**

103 The placental samples from three different sites were ground and mixed, then, total RNA

104 was isolated using TRIzol reagent (Invitrogen, CA, USA) according to the manufacturer's

105 protocol. Agarose gel electrophoresis and NanoDrop ND-1000 (Thermo Fisher Scientific,

106 MA, USA) was used to monitor RNA integrity and quality. Intact mRNA was isolated from

107 the total RNA samples using an Arraystar Seq-Star™ poly(A) Mrna Isolation Kit in

108 accordance with the manufacturer's protocol.

109 **Quantitative real-time PCR**

110 The expression of m6A-related genes *METTL3*, *METTL14*, *FTO*, *WTAP*, and *ALKBH5*

111 were detected by quantitative real-time PCR (RT-qPCR). Briefly, total RNA was isolated

112 using TRIzol reagent (Invitrogen), and cDNA was generated by reverse transcription

113 using Prime Script™ RT Master Mix (Perfect Real-Time; Takara Bio, Shiga, Japan). RT-

114 PCR was performed using SYBR Green master mix (Yeasen, Shanghai, China) and a

115 thermal cycler (LightCycler System; Roche Diagnostics Corp, IN, USA). β-Actin was

116 used as an internal control to normalise the data. The primers used for RT-qPCR are

117 presented in Table 2.

118 **Quantification of m6A in total RNA**.

119 The m6A RNA methylation status was directly detected using the EpiQuik™ m6A RNA

120 Methylation Quantification Kit (Colorimetric) according to the manufacturer's protocol.

121   Briefly, a negative control and a standard curve consisting of six different concentrations

122   (range: from 0.02 to 1 ng of m6A) were prepared. Two hundred nanograms of total RNA

123   was used for each reaction. After RNA binding to the 96-well plates, the binding solution

124   was removed and the plates were washed three times with diluted wash buffer. Then,

125   diluted capture anti-m6A antibodies were added; subsequently, the plates were washed

126   four times with diluted wash buffer. Add 100 μl of developer solution to each well and

127   incubate at room temperature for 7 min away from light. Add 100 ul of stop solution to

128   each well to stop enzyme reaction. The optical density (OD) at 450 nm was measured

129   using a microplate reader (BIOTEK, Vermont, USA). The absolute amount of m6A was

130   quantified, and the percentage of m6A within the total RNA was calculated.

131   **m6A-RIP-seq and data analysis**

132   Poly(A) RNA was extracted with Arraystar Seq-Star™ poly(A) mRNA Isolation Kit

133   (Arraystar, MD, USA). The RNA was fragmented into fragments with an average length

134   of 100 nt   using RNA Fragmentation Reagents (Sigma, MO, USA). Fragmented mRNAs

135   were incubated for 2 h at 4 °C in the presence of 2 μg m6A antibodies (Synaptic Systems,

136   202003) in a 500 μl IP reaction system, and some of the fragments were used as input.

137   The mixture was then incubated with protein-A beads and purified using elution buffer

138   and ethanol. RNA-seq libraries for m6A antibody-enriched mRNAs and input mRNAs

139   were prepared using the KAPA Stranded mRNA-seq Kit (Illumina, CA, USA). Finally, the

140   completed libraries were assessed using an Agilent 2100 Bioanalyzer. The libraries were

141   denatured with 0.1M NaOH and loaded into the reagent cartridge. Clusters were

142   generated using an Illumina cBot system (#PE-410-1001, Illumina). Sequencing was

143   performed on an Illumina HiSeq 4000 machine following HiSeq 3000/4000 SBS Kit (300

144   cycles) protocols.Quality control of the sequence data was performed using FastQC

145   (v0.11.7). The raw data were trimmed using Trimmomatic software (v0.32) and aligned

146   to the Ensembl reference genome using HISAT2 software (v2.1.0). The m6a-RIP-

147   enriched regions (peaks) were detected using exomePeak software (v2.13.2). The

148   differential m6A peaks (fold changes ≥1.5 and p < 0.05) between the case group and

149   control group were analysed using exomePeak. These differential peaks were annotated

150   using the Ensembl database (GRCh 37/hg19). DREME motif discovery in transcription

151   factor ChIP-seq data was used to identify motifs among the m6A peak sequences. Gene

152   ontology (GO) terms and Kyoto encyclopedia of genes and genomes (KEGG) pathways

153   were analyzed through GO database and KEGG pathway database.

154   **RNA-Sequencing**

155   Intact mRNA was isolated from total RNA samples using a NEBNext Poly(A) mRNA

156   Magnetic Isolation Module (New England Biolabs, Hertfordshire, UK) according to the

157   manufacturer's protocol. RNA-Seq libraries were prepared using a KAPA Stranded RNA-

158   Seq Library Prep Kit (Illumina). Sequencing was performed using the Illumina HiSeq

159   4000 platform.

160   **Quantifies m6A levels of *HSPA1A* using MazF-qPCR**

161   A previously reported strategy was adopted to identify m6A levels using the methyl-

162   sensitivity of MazF RNA endonuclease, which was previously shown to cleaves RNA at

163   unmethylated ACA sites, but not at sites with m6A methylation (Zhang et al. 2019).

164   500ng RNA was denatured by heating at 70°C for 2 min, then placed on ice. Each tube

165   was supplemented with 2 μl 5x MazF buffer, 1 μl mRNA interferase-MazF(TakaRa,

166   20U/ul), 1 μl RNase inhibitor, and DEPC-treated water was added to the total volume of

167   10 ul. After mixing, the mixtures were incubated at 37°C for 30 min and put on ice for

168   later use. MazF digested RNA (MazF +) and RNA without digestion (MazF -) was

169   reverse-transcribed into cDNA using Prime ScriptTM RT Master Mix (Takara Bio, Shiga,

170   Japan). RT-qPCR adopted the same method as described above, and the data were

171   analyzed by $2^{-\triangle\triangle CT}$ method. The m6A methylation at that particular site of *HSPA1A* was

172   the expression of *HSPA1A* with MazF treatment, which was normalized by MazF -.

173   *HSPA1A* primer set: Fwd: 5'AGGCCGACAAGAAGAAGGTG3', Rev:

174   5'CCTGGTACAGTCCGCTGATG3'.

175   **RT-qPCR of *HSPA1A* mRNA**

176   *HSPA1A* mRNA was quantified by RT-qPCR, which adopted the same method as

177   described above, and the primers used for RT-qPCR are presented in Table 2.

178   **Western blot analysis**

179   Western blot (WB) was performed in 4 PE samples and 4 control samples using

180   placental tissues. Briefly, protein was extracted from placental samples by the methods

181   of TRIzol. Block the membrane with 5% skim milk in Tris-Buffered Saline Tween-20

182   (TBST) for 1 hour. Primary antibody was used in 5% bovine serum albumin (BSA) and

183   incubated at room temperature for 2 h, then washed the membrane with TBST for 4

184   times, 8 min each time. The secondary antibody was incubated for 1.5 hour, and the

185   membrane was washed with TBST for 3 times. Membrane blots were visualized using

186   ECL plus detection kit (Thermo Fisher Scientific) and imaged on ImageQuant 4600

187   (Tenon, Shanghai, China).

188   **Statistical analyses**

189   Data are expressed as the mean ± standard deviation (SD). All statistical analyses were

190   conducted using the SPSS 22.0 statistical package. Student's t-test was used to

191   compare m6A, mRNA and protein levels between the PE and control samples. Fisher's

192   exact test was used for all bioinformatic analyses, and a p-value < 0.05 was considered

193   statistically significant.

194   ## Results

195   **The main clinical information of samples**

196   The main clinical data of the PE cases and controls are summarised in Table 1. All

197   women did not have diabetes, chronic hypertension, polycystic ovarian syndrome,

198   kidney or liver disease, and serious infection. Blood pressure and proteinuria were

199   significantly higher in the PE cases than in the controls. There was no significant

200   difference in maternal age, gestational age, prenatal maternal body mass index, and

201   birth weights at delivery between the groups.

202   **METTL3 and METTL14 were up-regulated in PE**

203   The concentration, purity and integrity of extracted RNA was shown in Table S1 and

204   Figure S1. Using qRT-PCR, we examined the mRNA levels of five core enzymes

205   responsible for m6A modification, including METTL3, METTL14, FTO, WTAP, and

206   ALKBH5, in the PE and control samples. mRNA levels of METTL3 and METTL14, the

207   key m6A methyltransferase, were significantly increased in the PE samples compared to

208   the control (Fig. 1; METTL3 p = 0.023; METTL14 p = 0.016). WTAP and the erasers FTO

209   and ALKBH5 were not significantly dysregulated in the PE group (Fig. 1).

210   **m6A modification profiles in PE**

211   In this study, each sample was generated nearly 20 M m6A-RIP-seq reads, and the

212   quality control metrics of the sequence data are shown in Table S2. The level of m6A

213   RNA methylation within the total RNA in the PE was higher than that in the controls (Fig.

214   2). We then analysed the genome-wide profiling of the m6A-modified mRNA in the PE

215   and control samples (GEO accession number: GSE143966). In total, 370 m6A peaks

216   were significantly up-regulated, whereas 315 peaks were down-regulated (fold changes

217   ≥1.5 and p < 0.05; Fig. 3A). The top 20 altered methylated m6A peaks are listed in Table

218   3, and all significantly differentially expressed m6A peaks are listed in Table S3.

219   Additionally, 203 genes have up-regulated m6A peaks, and 202 genes have down-

220   regulated m6A peaks (fold changes ≥1.5 and p < 0.05; Table S3). Each gene may have

221   one or more modified peaks. The identified m6A peaks were primarily enriched within the

222   coding sequence in proximity to the stop codons and in the 3′UTR (Fig. 3B, C & D).

223   Additionally, the m6A peaks were characterised by the canonical RRACH motif (R

224   represents purine, A is m6A, and H is a non-guanine base; Fig. 3E). *HSPA1A*, a

225 representation of the significantly up-regulated peak, is shown in Figure 3F, Figure 3G

226 and Supplemental Fig S2.

227 **GO analysis and pathway analysis of differentially methylated mRNA**

228 To investigate the functional physiological and pathological significance of m6A

229 modification in PE, GO functional analysis and KEGG pathway analysis were used to

230 examine the altered m6A peaks. GO analysis (the count of genes involved in a GO term

231 > 2, p < 0.05) revealed that the up-regulated peaks in PE were significantly involved in

232 macromolecule metabolic processes and the maintenance of DNA repeat elements,

233 nuclear and intracellular processes, and damaged DNA binding and heat shock protein

234 binding (Fig. 4A). The down-regulated peaks were significantly associated with organelle

235 organisation and membrane docking, intracellular and intracellular organelle functions,

236 and damaged DNA binding and cysteine-type endopeptidase activity involved in the

237 execution phase of apoptosis (Fig. 4B).

238   KEGG pathway analysis demonstrated that the up-regulated peaks in the PE group

239 were significantly associated with the Wnt signalling pathway, the mTOR signalling

240 pathway, and the AMPK signalling pathway (Fig. 4C). The down-regulated peaks were

241 significantly associated with amino sugar and nucleotide sugar metabolism (Fig. 4D).

242 **Overview of transcriptome profiles and conjoint analysis of m6A-RIP-seq and**

243 **RNA-seq data**

244 In this study, each sample was generated nearly 20 M RNA-seq reads, and the quality

245 control metrics of the RNA-seq data are shown in Table S2. Transcriptome profiles of the

246 altered genes in PE were determined by RNA-seq (GEO accession number:

247 GSE143953). Significantly differentially expressed genes (fold change ≥1.5 and p < 0.05)

248 between the PE and control samples were identified using a volcano plot (Fig. 5A); these

249 included 68 up-regulated and 52 down-regulated genes. The top twenty altered genes

250 are listed in Table 4. The top ten GO and pathways associated with the up- or down-

251 regulated genes are displayed in Supplemental Fig. S3. Hierarchical cluster analysis was

252 performed to identify differentially expressed genes between the two groups (Fig. 5B).

253 According to conjoint analysis of m6A-RIP-seq and RNA-seq data, all genes were

254 initially divided into four groups that included 55 hyper-methylated m6A peaks in mRNA

255 transcripts that were significantly up-regulated (30; hyper-up) or down-regulated (25;

256 hyper-down) and 50 hypo-methylated m6A peaks in mRNA transcripts that were

257 significantly up-regulated (34; hypo-up) or down-regulated (16; hypo-down) (Fig. 5D,

258 Table S4).

259 **The expression of *HSPA1A* is regulated by m6A modification**

260 In this study, we detected the m6A levels of *HSPA1A* at the particular site in the CDS

261 region were significantly upregulated in PE (Fig. 6A&B; *p* = 0.012). The particular site

262 include oligos "ACA" and "(m6A)CA", and the sequences were

263 5'GAAGGUGCUGGACAAGUGUCAAGA 3' and

264 5'GAAGGUGCUGG(m6A)CAAGUGUCAAGA3', respectively. Additionally, *HSPA1A*

265 mRNA and HSP70 protein expression was significantly increased in PE (Fig. 6C& D;

266 *HSPA1A* mRNA *p* = 0.048).

Discussion

It has long been accepted that placental structural and functional abnormalities can

cause a number of pregnancy-associated diseases such as PE, gestational diabetes

mellitus, intrauterine growth restriction, and gestational trophoblastic disease (Burton &

Jauniaux 2018; Burton et al. 2019; Chaiworapongsa et al. 2014; Mol et al. 2016;

Salomon et al. 2016; Veras et al. 2017). Portions of the placenta entering systemic

circulation cause maternal PE syndrome, which includes oxidative stress of the

syncytiotrophoblast and dysregulated uteroplacental perfusion (Burton et al. 2019;

Redman et al. 2014). PE is also associated with changes in placental DNA

methylation(Herzog et al. 2017) and gene expression (Junus et al. 2012; Liang et al.

2016). This study reveals a region-specific m6A methylation map, first, we found that

METTL3 and METTL14 were up-regulated in PE as determined by qPCR. Consistent

with this result, the total RNA m6A levels were increased in PE. Then, we identified

numerous m6A changes in PE placentas compared to healthy controls after excluding

the influence of maternal age, body mass index, perinatal complications, and gestational

age at diagnosis and delivery. A portion of the genes identified in this study were

previously associated with PE ; however, we also identified a number of novel genes.

Studies of the human placenta not only enrich our understanding of the mechanisms

underlying PE but also provide a theoretical basis for the prevention and pre-emptive

treatment of related diseases. Recent studies suggest that the placenta may play a

specific role in mediating the generation of intergenerational inheritance (Padmanabhan

288 et al. 2013). Therefore, an in-depth study of the placenta is crucial to determine the

289 mechanisms underlying developmental programming; any related interventions can not

290 only improve maternal and foetal health during pregnancy but also improve the health of

291 multiple generations.

292   m6A methylation plays a critical role in the regulation of coordinate transcriptional

293 and post-transcriptional gene expression   (Edupuganti et al. 2017; Fu et al. 2014; Liu et

294 al. 2017a; Piao et al. 2017; Wang et al. 2014; Yue et al. 2015; Zheng et al. 2017),

295 including mRNA splicing, export, localisation, translation, and stability. M6A within a

296 transcript can facilitate the binding of regulatory proteins and affect the potential of a

297 given transcript for translation. Recent studies have demonstrated a vital functional role

298 for m6A modification in promoting mRNA translation (Shi et al. 2017; Wang et al. 2015).

299 In this study, hundreds of abnormal m6A methylations were also found in the transcripts,

300 including within zinc finger transcription factors, which uncovers emerging links between

301 m6A mRNA methylation and genome transcription. Thus, RNA decoration by m6A in

302 these transcripts that promotes their interaction with nuclear transcription factors,

303 possibly conferencing recognition of these transcripts (Dominissini et al. 2012).

304   *HSPA1A* (heat shock protein 70, Hsp70) is a member of the chaperone machinery

305 that plays a central role in maintaining cellular homeostasis; this protein can elicit innate

306 and adaptive pro-inflammatory immune responses and reflect oxidative stress in PE

307 (Molvarec et al. 2011; Witkin et al. 2017), which is relevant to the progression of PE

308 (Chaiworapongsa et al. 2014). Interestingly, circulating Hsp70 can be directly involved in

309 endothelial activation or injury in PE (Molvarec et al. 2011; Witkin et al. 2017). Indeed, in

310 this study, we detected a significant increase in *HSPA1A* mRNA and protein expression

311 in PE. Furthermore, in a previous study, compared with normal pregnancy, Hsp70 was

312 significantly up-regulated in PE placental tissues (Molvarec et al. 2011; Sheikhi et al.

313 2015; Witkin et al. 2017). However, the exact mechanism of Hsp70 up-regulation in PE

314 remains unclear; it may be related to higher m6A methylation levels of *HSPA1A* in PE

315 placentas than those in the control samples. IGF2BPs are a distinct family of m6A

316 readers that promote the stability and storage of their target mRNAs and therefore affect

317 gene expression output (Huang et al. 2018). Moreover, 92% of the IGF2BP binding sites

318 are located in protein-coding transcripts and highly enriched in CDS near stop codons

319 and in 3'UTRs (Huang et al. 2018). Therefore, we concluded that the increase of m6a

320 methylation in the CDS region of *HSPA1A* may promote mRNA stability. In the present

321 study, we verified that the m6A levels in *HSPA1A* at the particular site in the CDS region

322 were significantly increased in PE using MazF-qPCR. Zhou et al. reported that the m6A

323 modifications of *HSPA1A* were increased at 5'UTR in mouse embryonic fibroblast (MEF)

324 cell line after heat shock stress (Zhou et al. 2015). Compared with this study, the two

325 studies have different species, different tissues, different cells and different treatment

326 process, which may be the reasons for the different results of two studies.   Further

327 studies are necessary to elucidate if Hsp70 expression is correlated with m6A

328 methylation of *HSPA1A* in human placenta*.*

329   KEGG pathway analysis revealed that these target genes were

330 significantly enriched in 20 different pathways, including the "Wnt signalling pathway",

331 "mTOR signalling pathway", "AMPK signalling pathway", and the others. Some of the

332 most essential and crucial pathological changes in the PE process include shallow

333 trophoblast invasion and the damaged spiral artery remodelling, which may be regulated

334 by Wnt/β-catenin signalling pathway (Zhang et al. 2017b). As a canonical Wnt-signalling

335 pathway, the Wnt/β-catenin signalling pathway can regulate several biological processes

336 such as proliferation, migration, invasion, and apoptosis (Nusse & Clevers 2017; Zhang

337 et al. 2017b). Abnormal functioning of the Wnt/β-catenin signalling pathway may play an

338 important role in the pathogenesis of various human diseases, including human cancer

339 and PE (Nusse & Clevers 2017; Zhang et al. 2017b); however, direct evidence of the role

340 of the Wnt/β-catenin pathway in the development of PE is lacking. In this study, genes

341 exhibiting abnormal m6A methylation were significantly enriched in the Wnt signalling

342 pathway; this may shed light on a new layer of gene regulation at the RNA level,

343 ultimately giving rise to the field of m6A epitranscriptomics. Interestingly, inhibition of

344 Wnt/β-catenin signalling is a promising treatment approach for a number of cancers

345 (Clara et al. 2019; Krishnamurthy & Kurzrock 2018; Nusse & Clevers 2017). Future

346 studies are recommended to verify if Wnt/β-catenin signalling may provide a prospective

347 therapeutic target for the prevention and treatment of PE.

348   In this study, 120 significantly differentially expressed genes were identified in PE,

349 some genes have been reported in previous studies, including *DIO2*, *BIN2*, *IGSF8*,

350 *BMP5*, and *WNT2* (Sitras et al. 2009; Zhang et al. 2016; Zhang et al. 2017b). These

351   genes, when differentially expressed in different populations, may play an important role

352   in the development of PE. Using bioinformatics analysis, differentially expressed genes

353   were enriched in biological processes involved in defence response, sphingolipid

354   metabolic processes, and tissue development, among others. Maternal-foetal immune

355   incompatibility and disruption of sphingolipid metabolism have emerged as factors

356   involved in the pathogenic mechanisms underlying PE (Chaiworapongsa et al. 2014;

357   Charkiewicz et al. 2017; Zhang et al. 2017b). This provides further evidence that PE is a

358   heterogeneous and multifactorial disease and that a variety of pathogenic mechanisms

359   are implicated in its occurrence and development.

360   Conjoint analysis of m6A-RIP-seq and RNA-seq data identified m6A-modified

361   mRNA transcripts that were hyper-methylated or hypo-methylated and significantly

362   differentially expressed. *TCF7L2*, a transcription factor of the Wnt and Hippo signalling

363   pathway, is hyper-methylated and up-regulated in PE, suggesting a possible positive

364   relationship between the extent of m6A methylation and the transcript level. Earlier

365   findings revealed that a *TCF7L2* variant increased the risk of incident hypertension or

366   diabetes mellitus (Bonnet et al. 2013; Chang et al. 2017); however, the relationship

367   between *TCF7L2* and PE is not clear. To provide further insight, it will be necessary, in a

368   future study, to elucidate the biological function of *TCF7L2* in the context of PE.

369   Gestational age is an important confounder when studying variation in placental

370   DNA methylation. Previous studies have illustrated gestational age as one of the

371   important factors that influence methylation (Novakovic & Saffery 2012; Wilson et al.

372   2018). Placentas obtained from preterm pregnant women with early PE were used in

373   some studies, to match gestational age, some placentas of women undergoing

374   spontaneous preterm delivery were used as control groups, which may possess

375   additional differences in methylation that are not detected at full-term (≥37 week

376   gestation) (Novakovic & Saffery 2012; Wilson et al. 2018; Yeung et al. 2016). In this

377   study, to exclude the influence of gestational age, we used full-term placentas obtained

378   from women with PE; however, we did not perform a study to determine that m6a

379   methylation changes with gestational age. This is a limitation of the present study.

380   **Conclusions**

381   Here, we describe, for the first time, the m6A RNA methylation landscape; reveal the

382   potential functions of this methylation in the regulation of RNA metabolism in PE.

383   Additionally, conjoint analysis of m6A-RIP-seq and RNA-seq data resulted in the

384   identification of differentially expressed hyper-methylated or hypo-methylated mRNA

385   m6A peaks. Finally, we uncovered that *HSPA1A* might be involved in the

386   pathophysiology of PE as its mRNA and protein expression is regulated by m6A

387   modification. Further studies will be necessary to validate more m6A-enriched genes and

388   examine protein levels of the genes which contribute to elucidate the detailed molecular

389   mechanism underlying the regulation and biological functions of m6A during the PE

390   process. Additionally, characterisation of the role of m6A within the placenta will offer a

391   new viewpoint to elucidate the mechanism of PE.

References

2019. ACOG Practice Bulletin No. 202: Gestational Hypertension and Preeclampsia. *Obstet Gynecol* 133:e1-e25.

Ahmed A, Rezai H, and Broadway-Stringer S. 2017. Evidence-Based Revised View of the Pathophysiology of Preeclampsia. *Adv Exp Med Biol* 956:355-374.

Bai Y, Rao H, Chen W, Luo X, Tong C, and Qi H. 2018. Profiles of circular RNAs in human placenta and their potential roles related to preeclampsia. *Biol Reprod* 98:705-712.

Boccaletto P, Machnicka MA, Purta E, Piatkowski P, Baginski B, Wirecki TK, de Crecy-Lagard V, Ross R, Limbach PA, Kotter A, Helm M, and Bujnicki JM. 2018. MODOMICS: a database of RNA modification pathways. 2017 update. *Nucleic Acids Res* 46:D303-D307.

Bonnet F, Roussel R, Natali A, Cauchi S, Petrie J, Laville M, Yengo L, Froguel P, Lange C, Lantieri O, Marre M, Balkau B, and Ferrannini E. 2013. Parental history of type 2 diabetes, TCF7L2 variant and lower insulin secretion are associated with incident hypertension. Data from the DESIR and RISC cohorts. *Diabetologia* 56:2414-2423.

Burton GJ, and Jauniaux E. 2018. Pathophysiology of placental-derived fetal growth restriction. *Am J Obstet Gynecol* 218:S745-S761.

Burton GJ, Redman CW, Roberts JM, and Moffett A. 2019. Pre-eclampsia: pathophysiology and clinical implications. *BMJ* 366:l2381.

Chaiworapongsa T, Chaemsaithong P, Yeo L, and Romero R. 2014. Pre-eclampsia part 1: current understanding of its pathophysiology. *Nat Rev Nephrol* 10:466-480.

Chang S, Wang Z, Wu L, Lu X, Shangguan S, Xin Y, Li L, and Wang L. 2017. Association between TCF7L2 polymorphisms and gestational diabetes mellitus: A meta-analysis. *J Diabetes Investig* 8:560-570.

Charkiewicz K, Goscik J, Blachnio-Zabielska A, Raba G, Sakowicz A, Kalinka J, Chabowski A, and Laudanski P. 2017. Sphingolipids as a new factor in the pathomechanism of preeclampsia - Mass spectrometry analysis. *PLoS One* 12:e0177601.

Chen X, Li X, Guo J, Zhang P, and Zeng W. 2017. The roles of microRNAs in regulation of mammalian spermatogenesis. *J Anim Sci Biotechnol* 8:35.

Clara JA, Monge C, Yang Y, and Takebe N. 2019. Targeting signalling pathways and the immune microenvironment of cancer stem cells - a clinical update. *Nat Rev Clin Oncol*.

Dominissini D, Moshitch-Moshkovitz S, Schwartz S, Salmon-Divon M, Ungar L, Osenberg S, Cesarkas K, Jacob-Hirsch J, Amariglio N, Kupiec M, Sorek R, and Rechavi G. 2012. Topology of the human and mouse m6A RNA methylomes revealed by m6A-seq. *Nature* 485:201-206.

Edupuganti RR, Geiger S, Lindeboom RGH, Shi H, Hsu PJ, Lu Z, Wang SY, Baltissen MPA, Jansen P, Rossa M, Muller M, Stunnenberg HG, He C, Carell T, and Vermeulen M. 2017. N(6)-methyladenosine (m(6)A) recruits and repels proteins to regulate mRNA homeostasis. *Nat Struct Mol Biol* 24:870-878.

Fu Y, Dominissini D, Rechavi G, and He C. 2014. Gene expression regulation mediated through reversible m(6)A RNA methylation. *Nat Rev Genet* 15:293-306.

Herzog EM, Eggink AJ, Willemsen SP, Slieker RC, Wijnands KPJ, Felix JF, Chen J, Stubbs A, van der Spek PJ, van Meurs JB, and Steegers-Theunissen RPM. 2017. Early- and late-onset preeclampsia and the tissue-specific epigenome of the placenta and newborn. *Placenta* 58:122-132.

Hiden U, Bilban M, Knofler M, and Desoye G. 2007. Kisspeptins and the placenta: regulation of trophoblast

432   invasion. *Rev Endocr Metab Disord* 8:31-39.

433   Huang H, Weng H, Sun W, Qin X, Shi H, Wu H, Zhao BS, Mesquita A, Liu C, Yuan CL, Hu YC, Huttelmaier S, Skibbe JR,
434   Su R, Deng X, Dong L, Sun M, Li C, Nachtergaele S, Wang Y, Hu C, Ferchen K, Greis KD, Jiang X, Wei M, Qu L,
435   Guan JL, He C, Yang J, and Chen J. 2018. Recognition of RNA N(6)-methyladenosine by IGF2BP proteins
436   enhances mRNA stability and translation. *Nat Cell Biol* 20:285-295. 10.1038/s41556-018-0045-z

437   Junus K, Centlow M, Wikstrom AK, Larsson I, Hansson SR, and Olovsson M. 2012. Gene expression profiling of
438   placentae from women with early- and late-onset pre-eclampsia: down-regulation of the angiogenesis-
439   related genes ACVRL1 and EGFL7 in early-onset disease. *Mol Hum Reprod* 18:146-155.

440   Krishnamurthy N, and Kurzrock R. 2018. Targeting the Wnt/beta-catenin pathway in cancer: Update on effectors
441   and inhibitors. *Cancer Treat Rev* 62:50-60.

442   Liang M, Niu J, Zhang L, Deng H, Ma J, Zhou W, Duan D, Zhou Y, Xu H, and Chen L. 2016. Gene expression profiling
443   reveals different molecular patterns in G-protein coupled receptor signaling pathways between early- and
444   late-onset preeclampsia. *Placenta* 40:52-59.

445   Liu N, Zhou KI, Parisien M, Dai Q, Diatchenko L, and Pan T. 2017a. N6-methyladenosine alters RNA structure to
446   regulate binding of a low-complexity protein. *Nucleic Acids Res* 45:6051-6063.

447   Liu X, Chen H, Kong W, Zhang Y, Cao L, Gao L, and Zhou R. 2017b. Down-regulated long non-coding RNA-ATB in
448   preeclampsia and its effect on suppressing migration, proliferation, and tube formation of trophoblast
449   cells. *Placenta* 49:80-87.

450   Ma JZ, Yang F, Zhou CC, Liu F, Yuan JH, Wang F, Wang TT, Xu QG, Zhou WP, and Sun SH. 2017. METTL14 suppresses
451   the metastatic potential of hepatocellular carcinoma by modulating N(6) -methyladenosine-dependent
452   primary MicroRNA processing. *Hepatology* 65:529-543.

453   Magee LA, Pels A, Helewa M, Rey E, and von Dadelszen P. 2014. Diagnosis, evaluation, and management of the
454   hypertensive disorders of pregnancy: executive summary. *J Obstet Gynaecol Can* 36:416-441.

455   Meyer KD, and Jaffrey SR. 2014. The dynamic epitranscriptome: N6-methyladenosine and gene expression control.
456   *Nat Rev Mol Cell Biol* 15:313-326.

457   Mol BWJ, Roberts CT, Thangaratinam S, Magee LA, de Groot CJM, and Hofmeyr GJ. 2016. Pre-eclampsia. *Lancet*
458   387:999-1011.

459   Molvarec A, Szarka A, Walentin S, Beko G, Karadi I, Prohaszka Z, and Rigo J, Jr. 2011. Serum heat shock protein 70
460   levels in relation to circulating cytokines, chemokines, adhesion molecules and angiogenic factors in
461   women with preeclampsia. *Clin Chim Acta* 412:1957-1962.

462   Muller-Deile J, Schroder P, Beverly-Staggs L, Hiss R, Fiedler J, Nystrom J, Thum T, Haller H, and Schiffer M. 2018.
463   Overexpression of preeclampsia induced microRNA-26a-5p leads to proteinuria in zebrafish. *Sci Rep*
464   8:3621.

465   Myatt L, and Webster RP. 2009. Vascular biology of preeclampsia. *J Thromb Haemost* 7:375-384.

466   Nikuei P, Rajaei M, Malekzadeh K, Nejatizadeh A, Mohseni F, Poordarvishi F, Ghashghaeezadeh N, and Mohtarami
467   M. 2017. Expression of placental growth factor mRNA in preeclampsia. *Int J Reprod Biomed (Yazd)* 15:169-
468   174.

469   Novakovic B, and Saffery R. 2012. The ever growing complexity of placental epigenetics - role in adverse pregnancy
470   outcomes and fetal programming. *Placenta* 33:959-970.

471   Nusse R, and Clevers H. 2017. Wnt/beta-Catenin Signaling, Disease, and Emerging Therapeutic Modalities. *Cell*
472   169:985-999.

473   Padmanabhan N, Jia D, Geary-Joo C, Wu X, Ferguson-Smith AC, Fung E, Bieda MC, Snyder FF, Gravel RA, Cross JC,
474   and Watson ED. 2013. Mutation in folate metabolism causes epigenetic instability and transgenerational
475   effects on development. *Cell* 155:81-93.
476   Pereira AC, Paulo M, Araujo AV, Rodrigues GJ, and Bendhack LM. 2011. Nitric oxide synthesis and biological
477   functions of nitric oxide released from ruthenium compounds. *Braz J Med Biol Res* 44:947-957.
478   Piao M, Sun L, and Zhang QC. 2017. RNA Regulations and Functions Decoded by Transcriptome-wide RNA Structure
479   Probing. *Genomics Proteomics Bioinformatics* 15:267-278.
480   Redman CW, Sargent IL, and Staff AC. 2014. IFPA Senior Award Lecture: making sense of pre-eclampsia - two
481   placental causes of preeclampsia? *Placenta* 35 Suppl:S20-25.
482   Salomon C, Scholz-Romero K, Sarker S, Sweeney E, Kobayashi M, Correa P, Longo S, Duncombe G, Mitchell MD,
483   Rice GE, and Illanes SE. 2016. Gestational Diabetes Mellitus Is Associated With Changes in the
484   Concentration and Bioactivity of Placenta-Derived Exosomes in Maternal Circulation Across Gestation.
485   *Diabetes* 65:598-609.
486   Sheikhi A, Razdar S, Rahmanpour H, Mousavinasab N, Ganji HB, and Jafarzadeh A. 2015. Higher expression of
487   HSP70 and LOX-1 in the placental tissues of pre-eclampsia pregnancies. *Clin Exp Hypertens* 37:128-135.
488   Shi H, Wang X, Lu Z, Zhao BS, Ma H, Hsu PJ, Liu C, and He C. 2017. YTHDF3 facilitates translation and decay of N(6)-
489   methyladenosine-modified RNA. *Cell Res* 27:315-328.
490   Sitras V, Paulssen RH, Gronaas H, Leirvik J, Hanssen TA, Vartun A, and Acharya G. 2009. Differential placental gene
491   expression in severe preeclampsia. *Placenta* 30:424-433.
492   Taniguchi K, Kawai T, Kitawaki J, Tomikawa J, Nakabayashi K, Okamura K, Sago H, and Hata K. 2020.
493   Epitranscriptomic profiling in human placenta: N6-methyladenosine modification at the 5'-untranslated
494   region is related to fetal growth and preeclampsia. *FASEB J* 34:494-512. 10.1096/fj.201900619RR
495   Veras E, Kurman RJ, Wang TL, and Shih IM. 2017. PD-L1 Expression in Human Placentas and Gestational
496   Trophoblastic Diseases. *Int J Gynecol Pathol* 36:146-153.
497   Wang T, Xiang Y, Zhou X, Zheng X, Zhang H, Zhang X, Zhang J, He L, and Zhao X. 2019. Epigenome-wide association
498   data implicate fetal/maternal adaptations contributing to clinical outcomes in preeclampsia. *Epigenomics*
499   11:1003-1019.
500   Wang X, Lu Z, Gomez A, Hon GC, Yue Y, Han D, Fu Y, Parisien M, Dai Q, Jia G, Ren B, Pan T, and He C. 2014. N6-
501   methyladenosine-dependent regulation of messenger RNA stability. *Nature* 505:117-120.
502   Wang X, Zhao BS, Roundtree IA, Lu Z, Han D, Ma H, Weng X, Chen K, Shi H, and He C. 2015. N(6)-methyladenosine
503   Modulates Messenger RNA Translation Efficiency. *Cell* 161:1388-1399.
504   Wilson SL, Leavey K, Cox BJ, and Robinson WP. 2018. Mining DNA methylation alterations towards a classification
505   of placental pathologies. *Hum Mol Genet* 27:135-146.
506   Witkin SS, Kanninen TT, and Sisti G. 2017. The Role of Hsp70 in the Regulation of Autophagy in Gametogenesis,
507   Pregnancy, and Parturition. *Adv Anat Embryol Cell Biol* 222:117-127.
508   Wu F, Tian FJ, Lin Y, and Xu WM. 2016. Oxidative Stress: Placenta Function and Dysfunction. *Am J Reprod Immunol*
509   76:258-271.
510   Yang Y, Hsu PJ, Chen YS, and Yang YG. 2018. Dynamic transcriptomic m(6)A decoration: writers, erasers, readers
511   and functions in RNA metabolism. *Cell Res* 28:616-624.
512   Yeung KR, Chiu CL, Pidsley R, Makris A, Hennessy A, and Lind JM. 2016. DNA methylation profiles in preeclampsia
513   and healthy control placentas. *Am J Physiol Heart Circ Physiol* 310:H1295-1303.

514　Yue Y, Liu J, and He C. 2015. RNA N6-methyladenosine methylation in post-transcriptional gene expression
515　　　　regulation. *Genes Dev* 29:1343-1355.

516　Zhang M, Muralimanoharan S, Wortman AC, and Mendelson CR. 2016. Primate-specific miR-515 family members
517　　　　inhibit key genes in human trophoblast differentiation and are upregulated in preeclampsia. *Proc Natl*
518　　　　*Acad Sci U S A* 113:E7069-E7076.

519　Zhang S, Zhao BS, Zhou A, Lin K, Zheng S, Lu Z, Chen Y, Sulman EP, Xie K, Bogler O, Majumder S, He C, and Huang S.
520　　　　2017a. m(6)A Demethylase ALKBH5 Maintains Tumorigenicity of Glioblastoma Stem-like Cells by
521　　　　Sustaining FOXM1 Expression and Cell Proliferation Program. *Cancer Cell* 31:591-606.e596.

522　Zhang Z, Chen LQ, Zhao YL, Yang CG, Roundtree IA, Zhang Z, Ren J, Xie W, He C, and Luo GZ. 2019. Single-base
523　　　　mapping of m(6)A by an antibody-independent method. *Sci Adv* 5:eaax0250. 10.1126/sciadv.aax0250

524　Zhang Z, Wang X, Zhang L, Shi Y, Wang J, and Yan H. 2017b. Wnt/beta-catenin signaling pathway in trophoblasts
525　　　　and abnormal activation in preeclampsia (Review). *Mol Med Rep* 16:1007-1013.

526　Zheng Q, Hou J, Zhou Y, Li Z, and Cao X. 2017. The RNA helicase DDX46 inhibits innate immunity by entrapping
527　　　　m(6)A-demethylated antiviral transcripts in the nucleus. *Nat Immunol* 18:1094-1103.

528　Zhou J, Wan J, Gao X, Zhang X, Jaffrey SR, and Qian SB. 2015. Dynamic m(6)A mRNA methylation directs
529　　　　translational control of heat shock response. *Nature* 526:591-594. 10.1038/nature15377

530

Table 1(on next page)

Clinical information of samples used in the study.

1 **Table 1. Clinical information of samples used in the study.**

Characteristic	Preeclampsia (n=4)	Control (n=4)	P Value
Maternal age, year	29.5 ± 1.3	29 ± 0.8	0.54
Gestational age, week	37.9 ± 0.5	38.2 ± 0.4	0.41
Prenatal maternal body mass index, kg/m2	27.6 ± 1.2	27.7 ± 0.8	0.86
Diastolic pressure, mmHg	110.3 ± 7.1	80 ± 4.2	3.40E-04
Systolic pressure, mmHg	162.5 ± 4.8	124.5 ± 4.9	3.27E-05
Proteinuria,g/24h	4.1 ± 0.5	0 ± 0	4.08E-04
Birth weight, g	3567.3 ± 290.2	3339 ± 316.6	0.33

2

3

Table 2(on next page)

Sequences of primers used for qRT-PCR analysis of mRNA levels.

1   **Table 2. Sequences of primers used for qRT-PCR analysis of mRNA levels.**

Gene name	Primer	Sequence	Product size (bp)
METTL3	Forward	5' ACAGAGTGTCGGAGGTGATT 3'	201
	Reverse	5' TGTAGTACGGGTATGTTGAGC 3'	
METTL14	Forward	5' TGAGATTGCAGCACCTCGAT 3'	250
	Reverse	5' AATGAAGTCCCCGTCTGTGC 3'	
WTAP	Forward	5' CCTCTTCCCAAGAAGGTTCGAT 3'	238
	Reverse	5' GTTCCTTGGTTGCTAGTCGC 3'	
FTO	Forward	5' AATAGCCGCTGCTTGTGAG 3'	182
	Reverse	5' CCACTTCATCTTGTCCGTTG 3'	
ALKBH5	Forward	5' GCCGTCATCAACGACTACCA 3'	208
	Reverse	5' ATCCACTGAGCACAGTCACG 3'	
HSPA1A	Forward	5' CCACCATTGAGGAGGTAGATTAG3'	176
	Reverse	5' CTGCATGTAGAAACCGGAAAA3'	
β-actin	Forward	5' GTGGCCGAGGACTTTGATTG 3'	73
	Reverse	5' CCTGTAACAACGCATCTCATATT 3'	

2

3

Table 3(on next page)

The top 20 differently expressed m6A peaks in PE.

1 **Table 3. The top 20 differently expressed m6A peaks in PE.**

Gene name	fold change	Regulation	Chromosome	Peak start	Peak end	Peak region	P-value
HSPA1A	47.50	Up	GL000251.1	3294734	3294974	cds	5.13E-06
DMWD	18.38	Up	chr19	46293970	46294029	cds, utr3	1.82E-02
HYOU1	15.67	Up	JH159138.1	67181	68226	cds, utr3	5.62E-03
BRCA1	15.14	Up	chr17	41245740	41245861	cds	6.61E-03
NDUFB2	13.36	Up	chr7	140396821	140400705	utr5	4.79E-02
SLC39A1	13.09	Up	chr1	153939949	153940038	utr5	1.38E-02
HYOU1	13.00	Up	JH159138.1	67162	68237	cds, utr3	7.94E-03
SCAF11	13.00	Up	chr12	46322790	46322910	utr5	2.75E-02
SLC25A29	12.47	Up	chr14	100760163	100760343	utr5	2.63E-02
MID1IP1	9.99	Up	chrX	38663134	38663344	utr5	1.55E-02
SLC6A2	0.07	Down	chr16	55689515	55689784	utr5	1.41E-02
NPIPB6	0.08	Down	chr16	28353905	28354053	utr3, cds	7.59E-03
LEKR1	0.09	Down	chr3	156544207	156544506	utr5	1.38E-02
MBLAC2	0.09	Down	chr5	89769658	89769897	cds	2.19E-02
TSSK6	0.10	Down	chr19	19626179	19626300	cds, utr5	3.16E-02
LRRC3	0.10	Down	chr21	45877072	45877311	cds, utr3	3.47E-02
RSPO1	0.12	Down	chr1	38077963	38078322	utr3	4.90E-02
AC016586.1	0.13	Down	chr19	4041364	4041783	utr3	6.17E-03
TEX40	0.14	Down	chr11	64071267	64072238	cds, utr3	3.16E-02
RPP25	0.15	Down	chr15	75246876	75246966	utr3	4.90E-02

2

3

Table 4(on next page)

The top 20 differently expressed genes in PE.

PeerJ

1 **Table 4. The top 20 differently expressed genes in PE.**

| Gene name	Fold change	Regulation	Locus	Strand	p_value
AOC1	8.51	Up	chr7:150521715-150558592	+	5.48E-04
HLA-DRB5	4.45	Up	chr6:32485120-32498064	-	4.50E-02
DIO2	4.31	Up	chr14:80663870-80854100	-	4.09E-03
NOTUM	4.27	Up	chr17:79910383-79919716	-	3.34E-02
SPIN1	4.04	Up	chr9:91003334-91093609	+	1.26E-03
LAIR2	3.55	Up	chr19:55009100-55021897	+	3.46E-03
PLAC8	2.96	Up	chr4:84011201-84058228	-	2.89E-02
DCD	2.61	Up	chr12:55038375-55042277	-	4.97E-02
UPK1B	2.57	Up	chr3:118892364-118924000	+	2.42E-02
PTPRCAP	2.57	Up	chr11:67202981-67205538	-	3.48E-03
H2AFJ	0.67	Down	chr12:14927317-14930936	+	2.06E-02
AHSA2	0.67	Down	chr2:61404553-61418338	+	2.87E-02
B3GNT2	0.66	Down	chr2:62423248-62451866	+	2.51E-02
PAK1	0.66	Down	chr11:77032752-77185680	-	4.96E-02
TMEM14B	0.66	Down	chr6:10747992-10852986	+	8.71E-03
IMPA2	0.66	Down	chr18:11981024-12030882	+	2.68E-04
PKNOX2	0.65	Down	chr11:125034583-125303285	+	3.23E-04
SLC9A6	0.65	Down	chrX:135056000-135129428	+	1.21E-02
HIST4H4	0.63	Down	chr12:14920933-14924065	-	1.74E-02
ANKRD33	0.63	Down	chr12:52281744-52285448	+	1.61E-02

2

PeerJ

Figure 1

METTL3 and METTL14 were up-regulated in PE.

Quantitative real-time PCR was used to analysis the mRNA levels of METTL3, METTL14, FTO, WTAP, and ALKBH5 in the PE samples and samples from normal pregnant women. All p-values were calculated using Student's t-test. $*p < 0.05$ versus control group (n = 4 each). PE: preeclampsia.
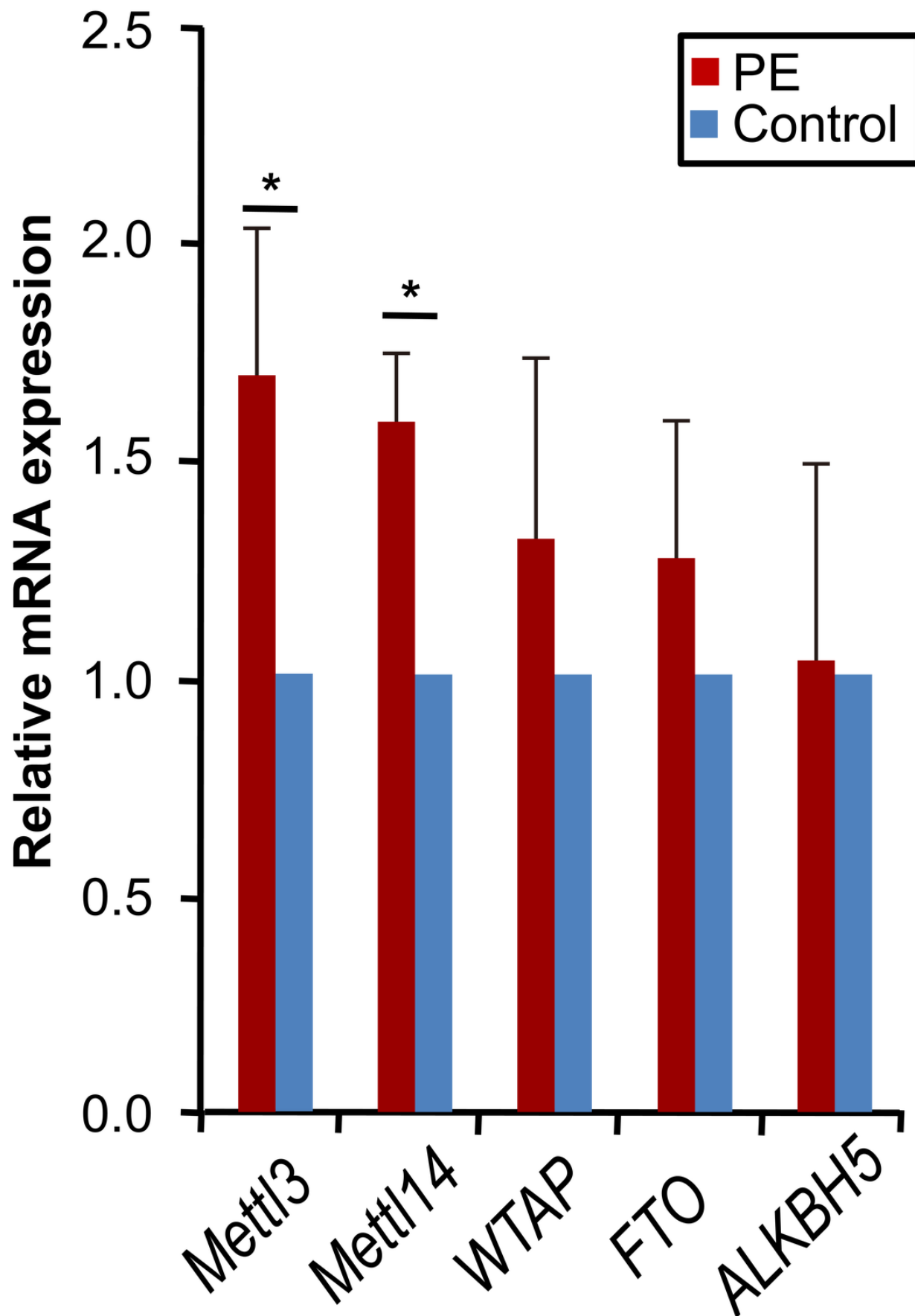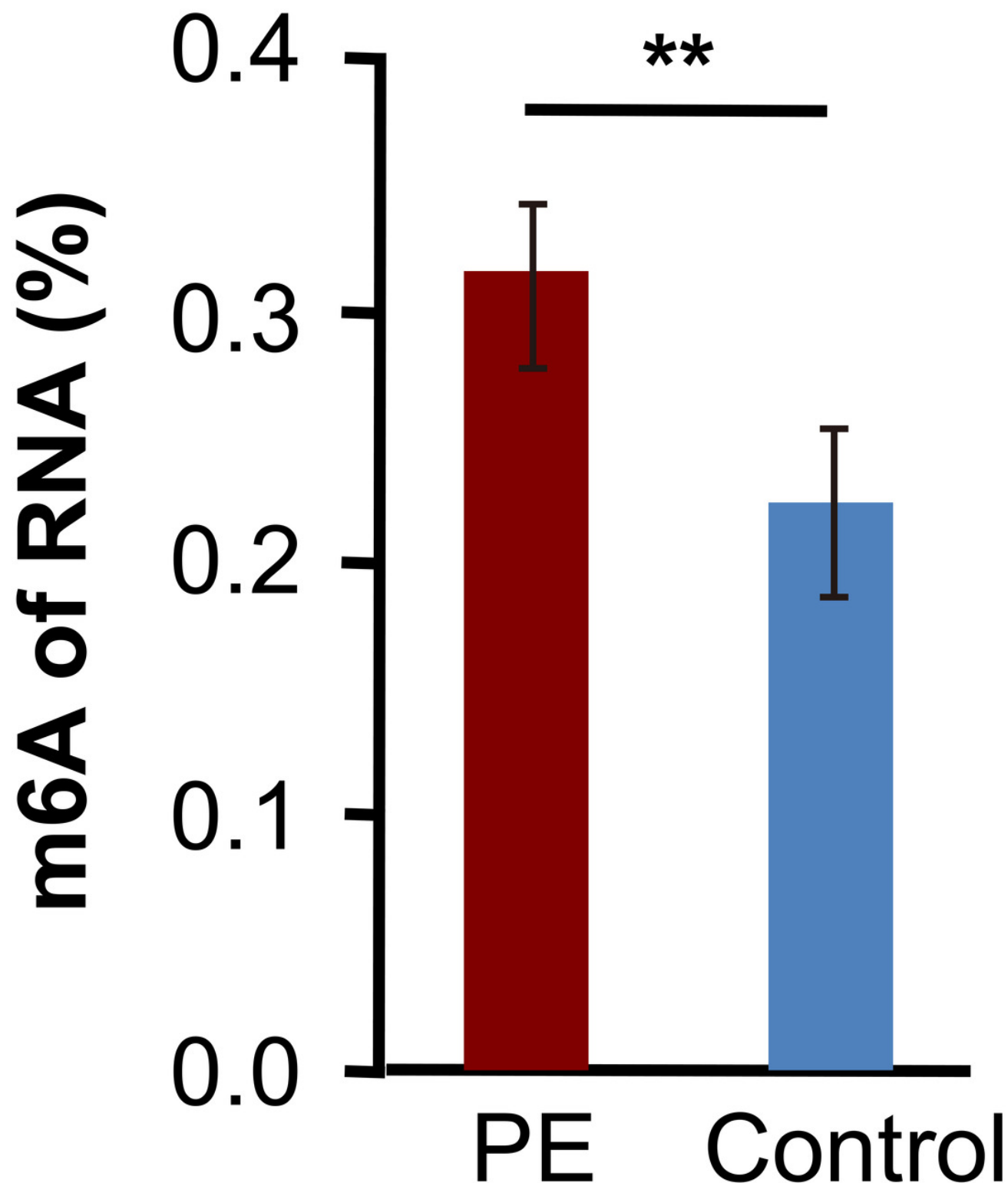
Figure 2

m6A levels of total RNA in PE and control.

m6A levels of total RNA were determined by antibody based colorimetric method. Data are presented as mean ± SD. All *p*-values were calculated using Student's t-test. **p < 0.01 versus control group (n = 4 each). PE: preeclampsia.

Figure 3

Overview of the m6A methylation landscape in the preeclampsia and control samples.

(A) Volcano plots displaying the distinct m6A peaks and their statistical significance (fold changes ≥1.5 and $p < 0.05$). (B) Metagene plots showing the region of average m6A peaks throughout the transcripts in the preeclampsia and control samples. (C) Pie charts displaying the distribution of m6A peaks in the preeclampsia. (D) Pie charts displaying the distribution of m6A peaks in the control group. (E) Sequence motifs of the m6A-containing peak regions. (F) Data visualisation analysis of *HSPA1A* mRNA m6A modifications in the preeclampsia group. (G) Data visualisation analysis of *HSPA1A* mRNA m6A modifications in the control group.
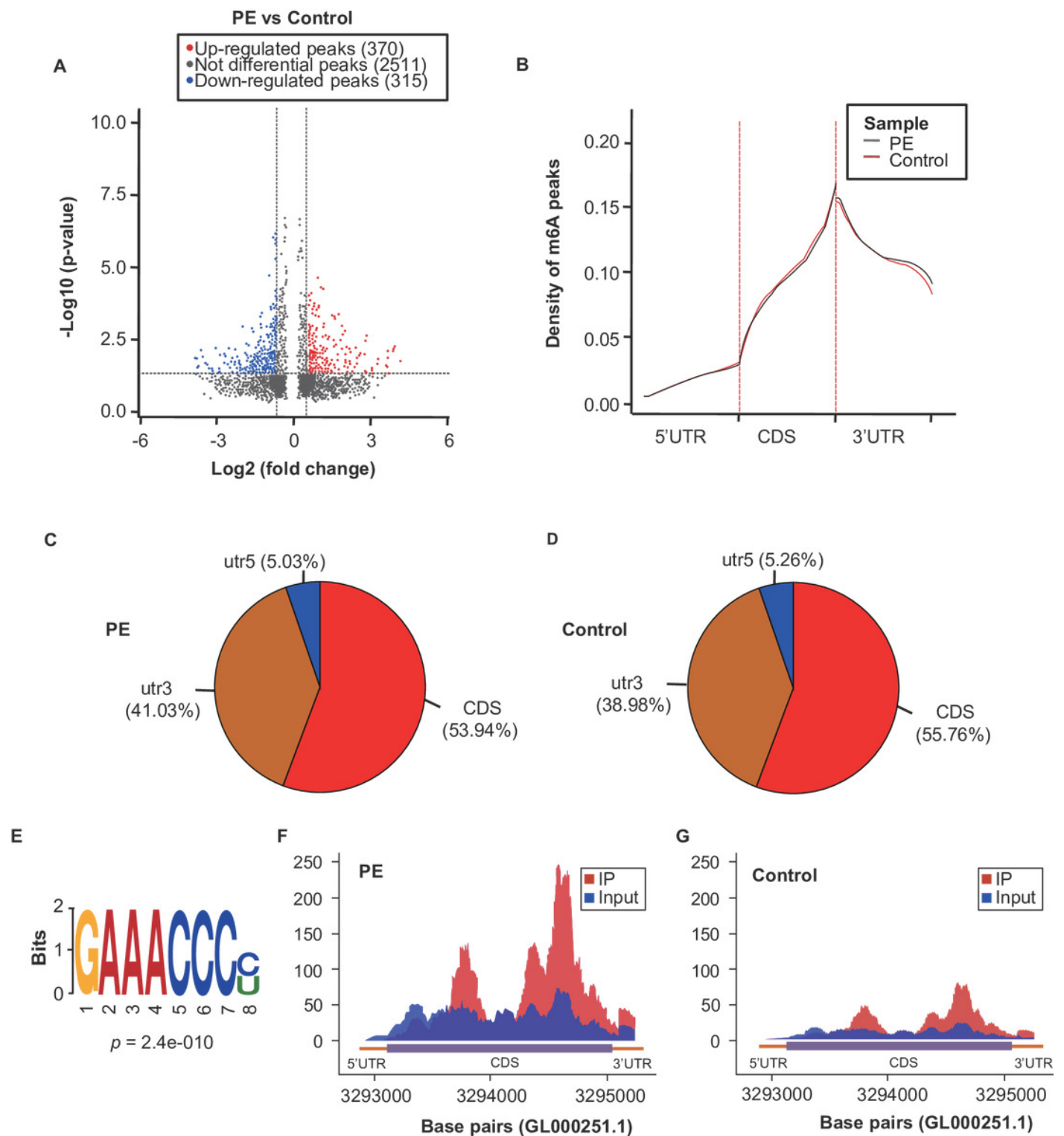
Figure 4

Gene ontology and KEGG pathway analyses of the altered m6A transcripts.

(A) Major enriched and significant GO-assessed up-regulated m6A peak transcripts. (B) Major enriched and significant GO-assessed down-regulated m6A peaks transcripts. (C) The top ten significantly enriched pathways for the up-regulated m6A peaks transcripts. (D) The top ten significantly enriched pathways for the down-regulated m6A peaks transcripts. GO: gene ontology, KEGG: Kyoto encyclopedia of genes and genomes, BP: biological process, CC: cellular component, MF: molecular function.
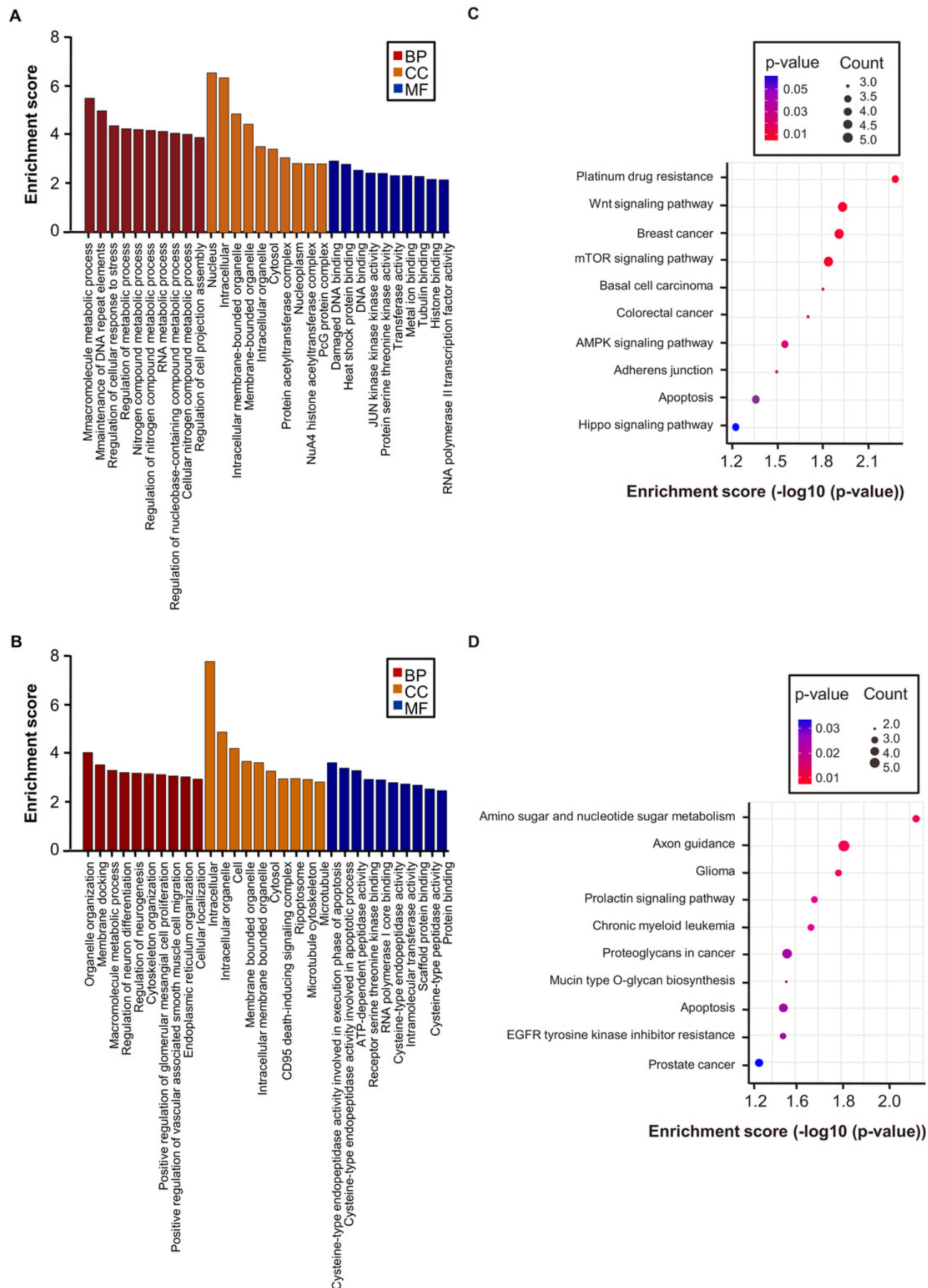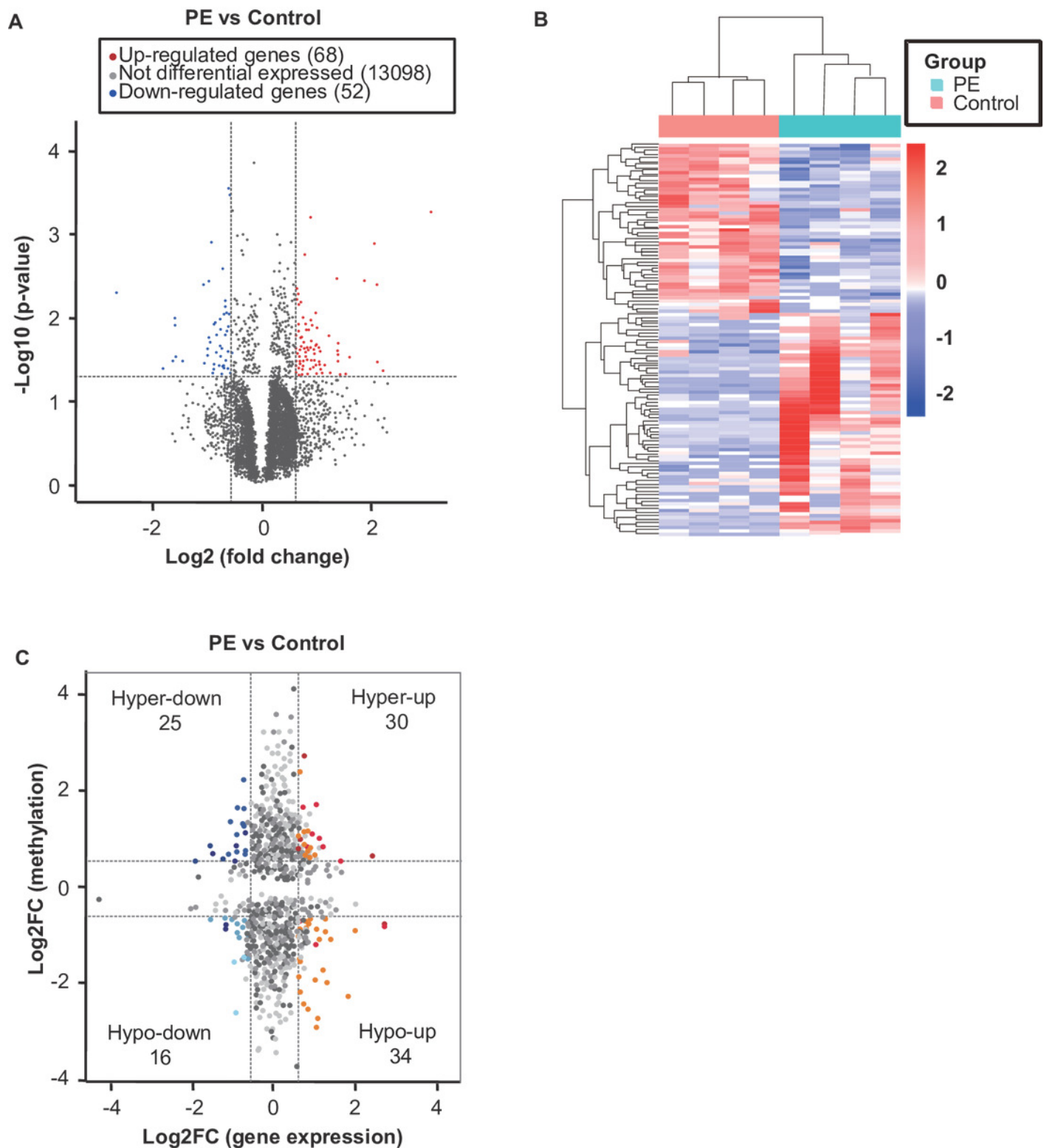
Figure 5

Conjoint analysis of m6A-RIP-seq and RNA-sequencing data for preeclampsia and controlsamples.

(A) Volcano plots displaying the mRNAs that were differentially expressed between the preeclampsia and control groups and their statistical significance (fold changes ≥1.5 and $p < 0.05$). (B) Hierarchical clustering analysis of the differentially expressed mRNAs. (C) Four quadrant graph showing the distribution of transcripts with a significant change in both m6A level and expression in preeclampsia.

Figure 6

The expression of *HSPA1A* is regulated by m6A modification.

(A) Schematic presentation of the location of verified m6A site in *HSPA1A*. (B) The m6A levels of *HSPA1A* at the particular site in the CDS region were significantly upregulated in PE. (C) The mRNA levels of *HSPA1A* were significantly increased in PE. (D) HSP70 protein expression was assessed by Western blot. All p-values were calculated using Student's t-test. *$p < 0.05$ versus control group (n = 4 each). PE: preeclampsia.